

# Numerical Simulation of the Bond Behavior between Concrete and Steel Reinforcing Bars in Specialty Concrete

Camille A. Issa, Omar Masri

**Abstract**—In this study, the commercial finite element software ABAQUS was used to develop a three-dimensional nonlinear finite element model capable of simulating the pull-out test of reinforcing bars from underwater concrete. The results of thirty-two pull-out tests that have different parameters were implemented in the software to study the effect of the concrete cover, the bar size, the use of stirrups, and the compressive strength of concrete.

The interaction properties used in the model provided accurate results in comparison with the experimental bond-slip results, thus the model has successfully simulated the pull-out test. The results of the finite element model are used to better understand and visualize the distribution of stresses in each component of the model, and to study the effect of the various parameters used in this study including the role of the stirrups in preventing the stress from reaching to the sides of the specimens.

**Keywords**—Bond strength, nonlinear finite element analysis, pull-out test, underwater concrete.

## I. INTRODUCTION

DESIGN and construction of underwater reinforced concrete structures requires comprehension of the bond behavior between the concrete and the steel reinforcing bars in order to achieve an adequate design. This bond is responsible for the transfer of longitudinal forces from the reinforcing bars to the concrete, and also for the behavior of crack opening in reinforced concrete members [1]. The performance of underwater concrete (UWC) is inferior to that of concrete cast above water due to aggregate segregation and washout loss.

Numerous investigations have attempted to study, experimentally and analytically, the bond behavior between concrete cast above water and steel reinforcement [2]-[4]. Other investigators have tried to understand the bond behavior through finite element modeling of the pull-out test [5]-[8]. ACI 408R-03 [2] stated that, for deformed bars, the forces transfer from steel bars to the surrounding concrete occurs through mechanical anchorage of the ribs, frictional forces due interface roughness, and chemical adhesion between the two materials. Various parameters were reported to have effects on the bond between and concrete. These parameters can be divided into three categories: structural characteristics such as concrete cover, bonded length of the bar, and others; bar

properties such as bar size, stress and yield strength of steel, and others; and concrete properties such as compressive strength, presence of admixtures, density, and others [2].

The bond behavior between UWC and steel reinforcement has been studied by few researchers over the last decades. Assaad and Issa [3] reported a remarkable difference between the bond stress-slip relationship of UWC and that obtained for concrete cast above water through reference mixtures. Among these researchers, none has attempted to create a finite element model of the pull-out test in UWC.

The primary objective of this paper is to develop a 3D nonlinear finite element model capable of simulating the experimental bond-slip relationship between reinforcing bars and UWC, thus providing an ability to study and visualize the level of stress transferred by the bond using finite modelling capabilities of ABAQUS. This visualization will help us to understand the effect of the concrete cover, the embedment length, and the use of stirrups on the distribution of stresses inside the specimen.

## II. EXPERIMENTAL PROGRAM

### A. Material Properties and Bond Parameters

The results of 32 pull-out tests are used in this paper. The concrete and steel properties for the 32 specimens are summarized in Table I. These specimens included different parameters that affect the bond-slip relationship as provided by the ACI 408R-03 [2]. The first category is the structural characteristics where the tested samples included different concrete covers (55 and 100 mm), an embedment length of 90 mm, and two stirrups as transverse reinforcements. The second category is the bar properties where four different bar sizes were tested. The last category is the concrete properties where four different compressive strengths ( $f'_c$ ) were used. Additionally, two underwater concrete admixtures were added to all specimens. The two added admixtures are a high-range water-reducing (HRWR) and an anti-washout admixture (AWA). Tables I and II provide a summary of these parameters.

### B. Specimen Preparation and Experimental Testing

The 32 specimens were cast in 250 mm depth rectangles with a height of 250 or 300 mm depending on the concrete cover. The steel bars were placed in the molds before casting with an embedded length of 90 mm. PVC bond breakers were also inserted at both sides of the embedment length. A universal testing machine was used to perform the pull-out test

Camille A. Issa, PhD, PE, F. ASCE, is a Professor of Civil Engineering at The Lebanese American University, Byblos, Lebanon. (Phone: 961-302-2682; fax: 961-994-4850; e-mail: cissa@lau.edu.lb).

Omar Masri was a Graduate Student in department of Civil Engineering at The Lebanese American University, Byblos, Lebanon.



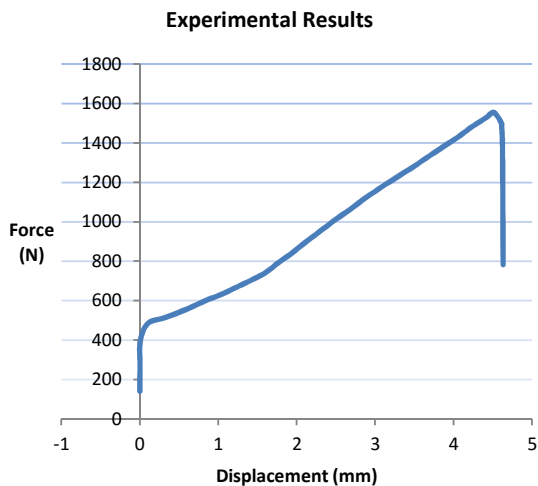


Fig. 4 Local force-displacement relationship for mix No. 5

TABLE III  
MATERIALS PROPERTIES FOR MIX NO. 5

Material	$E_c$ (GPa)	Density (Kg/m <sup>3</sup> )	Poisson's ratio
Concrete	25	2380	0.2
Steel	205	7800	0.3

*C. Load and Boundary Conditions*

To simulate the experimental results, the load applied on the steel bar consisted of an axial displacement applied at a distance equal to the upper LVDT position and in the pull-out direction. The imposed displacement, obtained and equal to the experimental displacement at the upper LVDT, generated the required force to pull the steel bar for some distance. The opposite direction of the steel bar was free to move. The time step of the simulation is equal to the experimental time span and is applied in small increments to overcome numerical instabilities. The concrete specimen was fixed at the surface in the pull-out direction and left free at all remaining surfaces. Fig. 5 presents the complete model for mix No. 5 showing the position of the applied displacement and the boundary conditions.

*D. Translators and Interaction Properties*

The most complex task in the modeling of the pull-out test is selecting the appropriate element that would accurately simulate the interaction between reinforcing bars and the surrounding concrete. Spring-like translators, which are one type of connectors available in ABAQUS, were used to simulate the transfer of forces from the reinforcement bars to the concrete. This type of connector has shown good results in modeling the pull-out test [8].

The translator is a type of connector that offers a slot constraint between two nodes in addition to aligning their local directions. A translator provides the best results when node b is placed at the center of the point enforcing the constraint as shown in Fig. 6 [15].

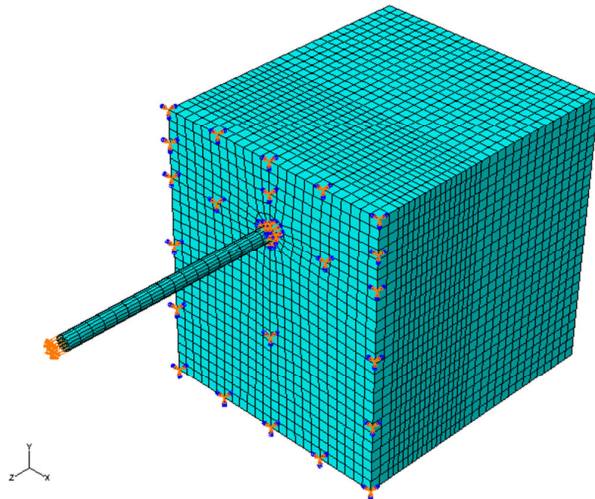


Fig. 5 Complete model for mix No. 5

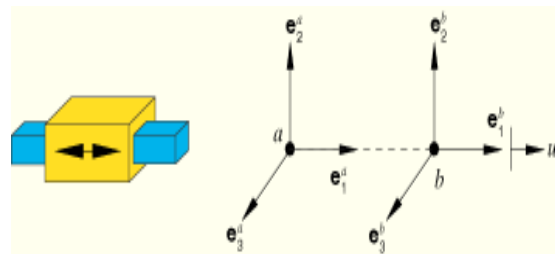


Fig. 6 Schematic of translator used [15]

By looking at Fig. 6, one can see the similar relationship between the yellow and blue parts from one side, and the concrete and reinforcement from another side. For the connector, translation is only allowed in the direction of the segment joining node “a” by node “b” or parallel to the axis of the blue part. These connectors were used to connect the common nodes between reinforcement and concrete along the embedded length of the rebar in the pull out direction.

Eight translators were introduced along the embedded length of the steel bar and four translators around the circumference as shown in Figs. 7 and 8. The translator behavior was defined as a spring like nonlinear elastic behavior. The connector data for the local force-displacement were obtained through dividing the experimental values by the total number of translators.

The translator was used only for the direction parallel to the rebar. However, for the direction perpendicular to the reinforcement, a hard contact interaction property was employed which involves a master-slave relationship between the rebar and the surrounding concrete. No interaction was employed for the un-bonded length and the reinforcement was free to move in this part.

The transverse reinforcements, stirrups, were modeled as solid embedded elements in the concrete specimen.

IV. RESULTS AND DISCUSSION

A. Numerical Analysis Results

To validate the model, a comparison has been made between the experimental bond-slip relationship and the one obtained through the numerical analysis. Fig. 9 provides the output of the comparison where the results were almost identical, which verifies that the finite element model could successfully simulate the pull-out experiment performed in the lab.

Table IV presents, by order, the maximum stress obtained in concrete and steel of each mix at the maximum force reached during the experiment. Clearly, the maximum stress in the concrete was obtained in the mix of the following characteristics: smallest bar diameter (12.7mm), largest concrete cover (10mm), and highest compressive strength (58MPa). However, apart from the mix with the highest stress in concrete, the results of the remaining mixes have no clear pattern and require further analysis. The maximum stress obtained in the steel bar at the maximum force is for the same mix that has the maximum stress in the concrete as shown in Table IV. Yet, the order of the maximum stress in concrete and steel is different for the remaining mixes.

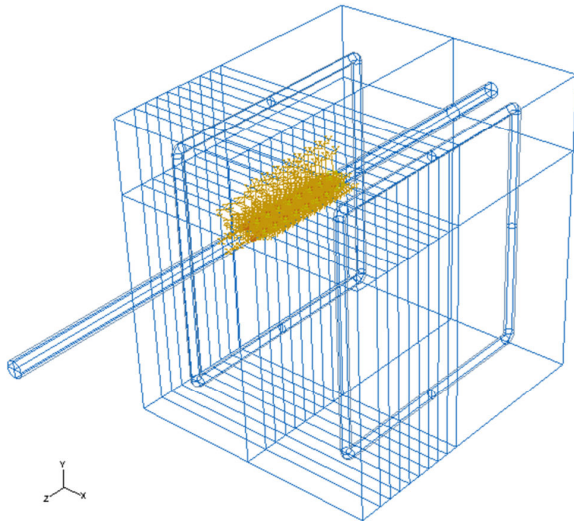


Fig. 7 Distribution of translators along the embedded length

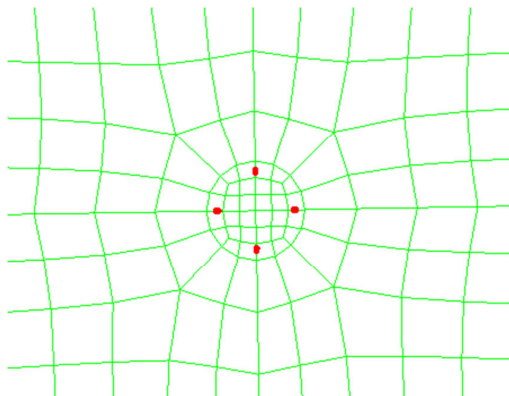


Fig. 8 Distribution of translators around the bar circumference

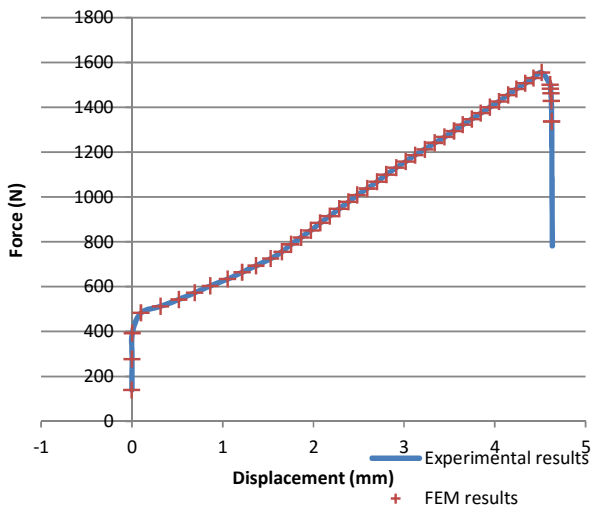


Fig. 9 Experimental vs. numerical bond-slip relationship

TABLE IV  
NUMERICAL ANALYSIS RESULTS

Mix No.	Maximum Stress (MPa)		Compressive strength (MPa)	Bar Diameter (mm)	Concrete Cover (mm)
	Concrete	Steel			
29	65.6	426.7	58	12.7	100
13	56.2	365.3	31	12.7	100
30	49.6	395.2	58	15.9	100
27	48.5	298.7	54	19.1	100
5	44.8	378.7	31	12.7	55
15	44	271.4	31	19.1	100
14	43.5	346.2	31	15.9	100
26	40.4	321.6	54	15.9	100
32	40.1	160.3	58	25.4	100
31	38.7	238.7	58	19.1	100
21	38.1	322.1	58	12.7	55
17	36.5	308.6	54	12.7	55
28	35.8	145.1	54	25.4	100
10	33.8	269.2	27	15.9	100
12	32.3	132.4	27	25.4	100
19	32.3	197.4	54	19.1	55
16	32	132	31	25.4	100
22	31.1	245.5	58	15.9	55
11	29.9	184.3	27	19.1	100
7	29.3	179.5	31	19.1	55
2	28.6	225.3	27	15.9	55
6	28.3	223.1	31	15.9	55
18	27.7	218.8	54	15.9	55
20	27	110	54	25.4	55
4	25.7	105.8	27	25.4	55
23	24.1	146.9	58	19.1	55
1*	23.5	199	27	12.7	55
9*	23.5	150.4	27	12.7	100
24	17.8	72.8	58	25.4	55
3	17.7	108.4	27	19.1	55
8	13.7	56.5	31	25.4	55
25*	-	-	54	12.7	100

\* Experimental errors have occurred

Few more remarks can also be drawn from Table IV such as: stress increased generally in the concrete when the bar diameter decreased or the concrete cover increased, concrete compressive strength  $f_c$  did not appear to have main influence on the results, and the rebar stress increased with the decrease of the steel bar diameter. The relation between these parameters will be studied in the next section.

*B. Effects of the Different Parameters on the Maximum Stress*

In order to study more the effect of each parameter (i.e. concrete cover, concrete compressive strength, and bar diameter) on the maximum stress inside the concrete specimens, the following charts were created through fixing two parameters and plotting the remaining parameter against the maximum stress in the concrete.

Fig. 10 combines the results of the maximum stress obtained in the concrete for specimens with a concrete cover of 55 mm and different  $f_c$  presented on the main axes. The variable parameter is the bar diameter. The plot illustrates that the highest stresses were obtained in the specimens with the smallest bar diameter (12.7mm). The only exception is in mix No. 1 due to experimental errors. For the remaining bar sizes, no clear relation can be concluded about the change in pattern.

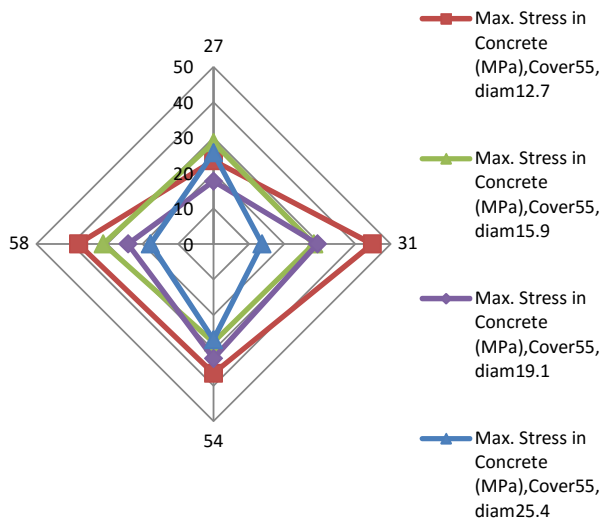


Fig. 10 Maximum stress in concrete for cover of 55 mm and variable parameters

For a concrete cover of 100 mm, similar relations were obtained as shown in Fig. 11. The highest stresses correspond to the specimens with the smallest bar diameter with no further relation for the remaining bar sizes.

Fig. 12 combines Figs. 10 and 11 to study the effect of increasing the concrete cover. It is clear from the plot that increasing the concrete cover will increase the maximum stress in the concrete specimen. For the sake of understanding the effect of the concrete compressive strength  $f_c$  on the maximum stresses in the concrete specimens and its correlation with the other two parameters, Figs. 13-15 were

plotted. Figs. 13 and 14 combine the results of the maximum stress obtained in the concrete for specimens with a concrete cover of 55 & 100 mm respectively and different bar sizes presented on the main axes. The variable parameter is the concrete compressive strength  $f_c$ . These two charts demonstrate that a pattern does not exist between these variables. In other terms, for each bar size, the maximum stresses obtained correspond to a different  $f_c$ .

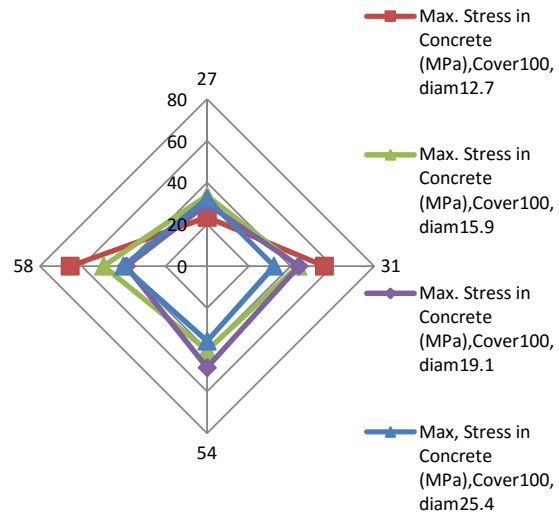


Fig. 11 Maximum stress in concrete for cover of 100 mm and variable parameters

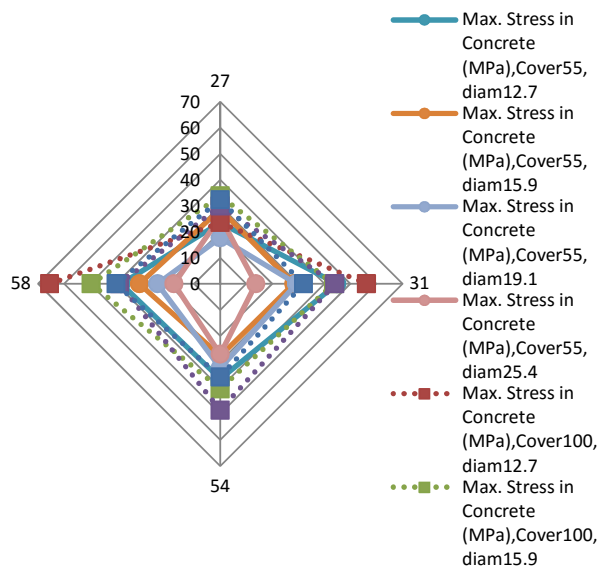


Fig. 12 Concrete cover effect

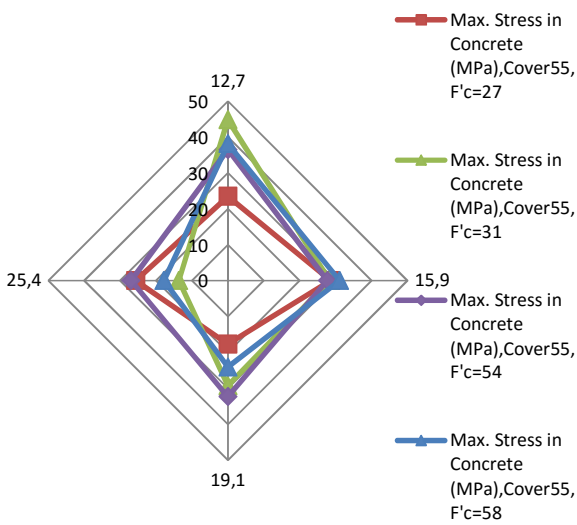


Fig. 13 Maximum stress in concrete for cover of 55 mm and variable parameters

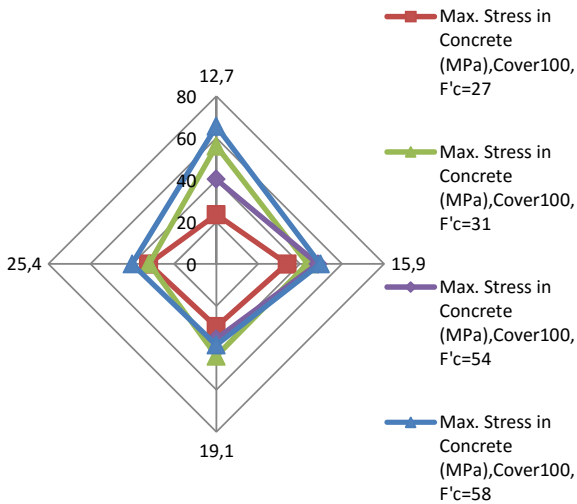


Fig. 14 Maximum stress in concrete for cover of 100 mm and variable parameters

*B. Stress Distribution in Different Components*

For the full specimen, the distribution of stresses at the maximum force is shown in Fig. 15. It can be observed that the maximum stresses are always obtained in the main steel bar.

The concrete is mainly in compression. But, by looking at the stress distribution inside only the concrete specimen as in Fig. 16, the effect of the bond in modifying the concrete stresses can be witnessed through the distortion of the stress contours around the bar location. The maximum stress is obtained in the region around the embedded length, and decreases in circular form towards the specimen extremities. Almost negligible stresses are obtained at the four corners in the back.

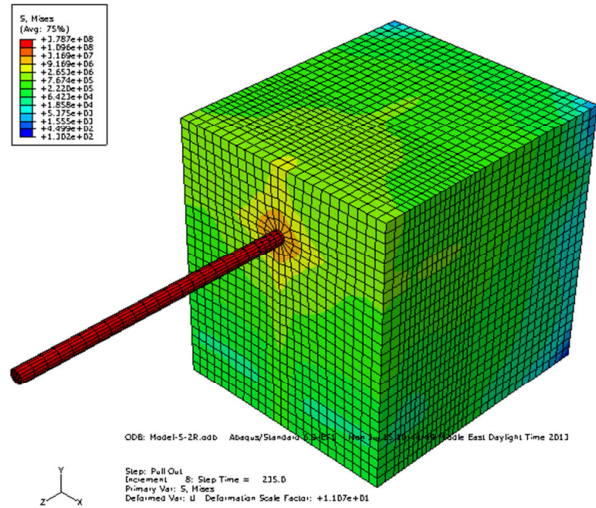


Fig. 15 Stress distribution for mix No. 5

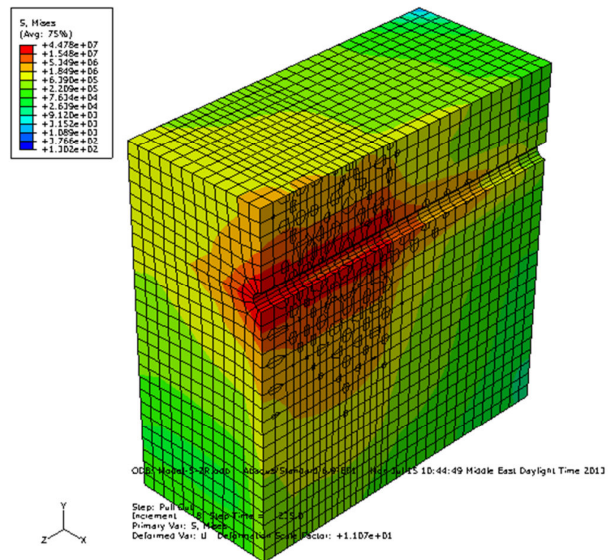


Fig. 16 Stress distribution in the concrete for mix No. 5 (vertical cut)

The steel bar is mainly in tension having the maximum stress value near the location of the applied load as can be seen if Fig. 17 and the stress level decreases gradually toward the opposite free end as it should be expected. The maximum stresses in the transverse reinforcements, stirrups, are occurring at the same height level of the rebar and from the inner surface. These stresses are shown in Fig. 18 for mix No. 5 and they have a maximum value of 24.5 MPa.

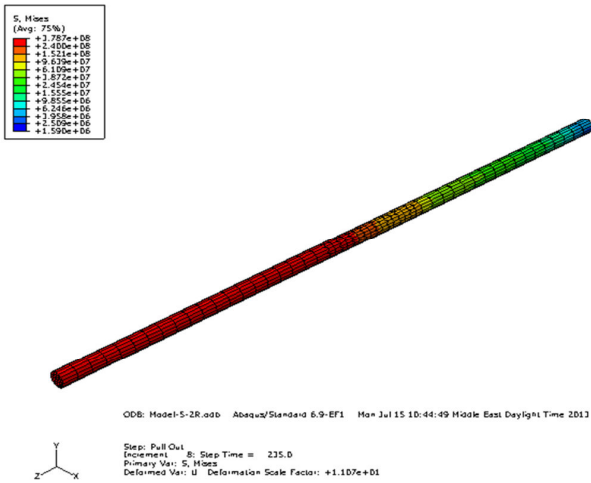


Fig. 17 Stress distribution in the steel bar for mix No. 5

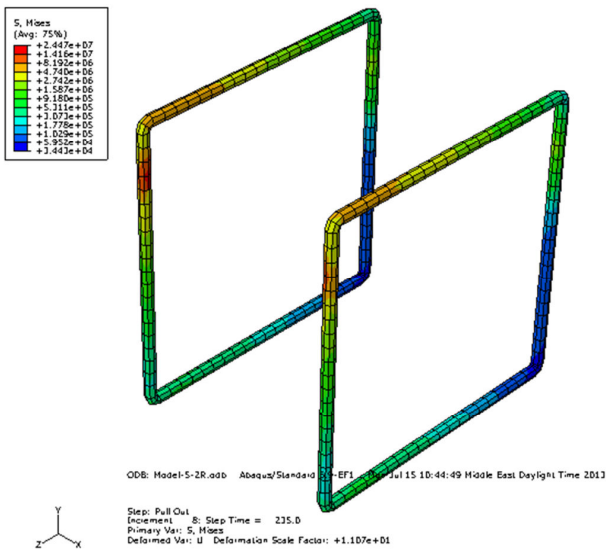


Fig. 18 Stress distribution in the stirrups for mix No. 5

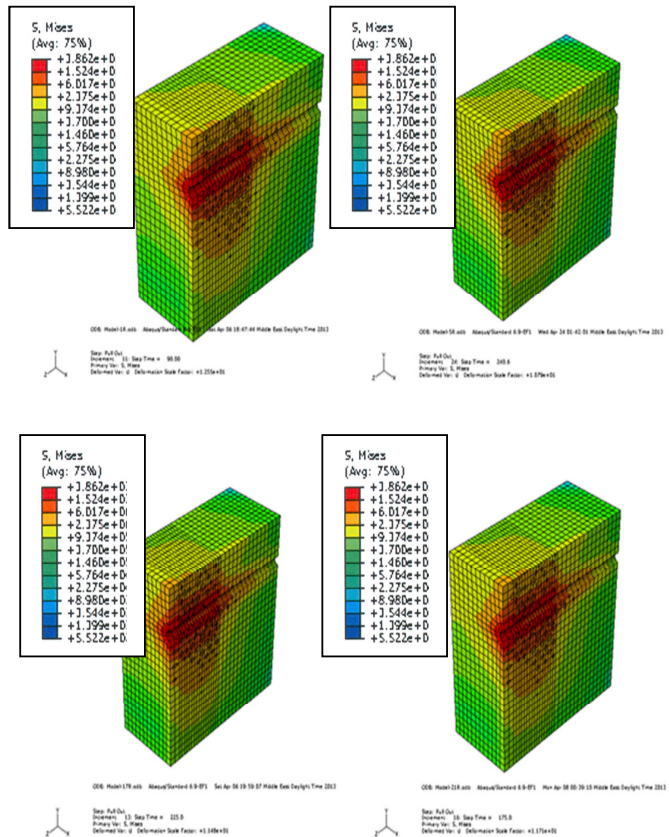


Fig. 19 Stress distribution in concrete for mix No. 1, 5, 17, and 21 respectively

*C. Analysis of the Stirrups Effects*

To understand the effect of the stirrups on the stress distribution inside the specimens, mix No. 31 was modeled with and without the transverse reinforcement. The results are provided in Figs. 20 and 21 respectively. It can be concluded from the results that using stirrups has limited the stress in the concrete specimen from propagating to the sides. The stirrups seem to absorb the stresses and limit its arrival to side parallel to the stirrups location. However, the maximum stress value in the concrete specimen surrounding the bonded length seems not to be affected or modified by the presence of the transverse reinforcement. Furthermore, almost the same stress value was achieved at the upper face of the concrete specimen but over a smaller area.

V. CONCLUSION

This research offers a step toward a better understanding of the stress distribution during the pull-out test in UWC. The main objective of this paper was to create a 3D nonlinear finite element model to simulate the experimental results of the pull-out test in UWC, and to study the stress distribution in each component using the commercial finite element software ABAQUS. Based on the obtained results, the FE model developed has successfully simulated the bond-slip relationship obtained through experimental test.

Fig. 19 corresponds for the distribution of stresses in specimens 1, 5, 17, and 21 respectively. These specimens share the same steel bar diameter of 12.7 mm and same the concrete cover of 55 mm, but each one has different concrete compressive strength  $f'_c$ . The stress contours in all these specimens are almost identical in terms of pattern, but differ only by values. Therefore, increasing the concrete compressive strength had no effect on the distribution of stresses in the concrete specimen. Similar results were obtained when comparing specimens with a concrete cover of 100 mm.

In comparison of the four different specimens, the highest stress that has been transferred from the rebar to concrete surface was obtained in mix No. 5 where the stress at the top surface of the concrete reached a value of 5.5 MPa. The experimental testing of these four specimens showed that only mix No. 5 suffered a crack that is perpendicular to the steel bar in the direction of the maximum stress.

